Volume 1 | Number 1 | Jan 2013 | Pages 1–100

Dalton Transactions

An international journal of inorganic chemistry
www.rsc.org/dalton

ROYAL SOCIETY OF CHEMISTRY

This is an *Accepted Manuscript*, which has been through the Royal Society of Chemistry peer review process and has been accepted for publication.

Accepted Manuscripts are published online shortly after acceptance, before technical editing, formatting and proof reading. Using this free service, authors can make their results available to the community, in citable form, before we publish the edited article. We will replace this *Accepted Manuscript* with the edited and formatted *Advance Article* as soon as it is available.

You can find more information about *Accepted Manuscripts* in the **Information for Authors**.

Please note that technical editing may introduce minor changes to the text and/or graphics, which may alter content. The journal's standard **Terms & Conditions** and the **Ethical guidelines** still apply. In no event shall the Royal Society of Chemistry be held responsible for any errors or omissions in this *Accepted Manuscript* or any consequences arising from the use of any information it contains.

ROYAL SOCIETY OF CHEMISTRY

www.rsc.org/dalton

TOC

A dimanganese complex containing a redox-active elongated disulfide bond electrocatalyses proton reduction.

Journal Name
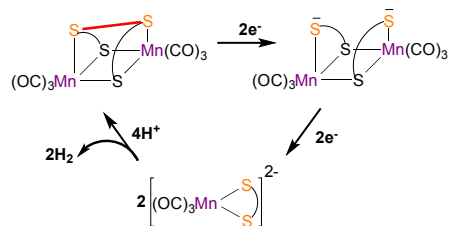
COMMUNICATION

Electrocatalytic Proton Reduction Catalyzed by A Dimanganese Disulfide Carbonyl Complex Containing a Redox-active Internal Disulfide Bond

Kaipeng Hou, Wai Yip Fan*

A dimanganese hexacarbonyl complex [(Mn(CO)$_3$)$_2$(μ-SC$_6$H$_4$-o-S-S-C$_6$H$_4$-o-μ-S-)] containing an elongated disulfide bond electrocatalyses proton reduction at moderate overpotentials of 0.55 to 0.65V. Cyclic voltammetric, infrared spectroscopy and computational studies suggest that the redox-active sulfur atoms of the disulfide bond serve as the initial reduction site.

Since crystallographic methods revealed that the Fe$_2$S$_2$ core was essential to the function of [FeFe]hydrogenase,[1] hundreds of synthetic models have been prepared to mimic the active site of the hydrogenase.[2-4] Among the model complexes, the electrocatalytic proton reduction performance of benzenedithiolate ligands bridged diiron complexes has been evaluated.[5] An iron hydride intermediate was proposed to act as a hydride donor and reacted with the acid to generate dihydrogen heterolytically. This mechanism was further supported by other reports where iron hydride complexes were characterized by X-ray crystallographic methods.[6-8]

Although many diiron catalysts have been used as hydrogenase mimics, dimanganese model complexes have so far not been reported. Our group has shown that thiols could be transformed into disulfides and H$_2$ using Mn(CO)$_5$Br or CpMn(CO)$_3$ under uv-visible light.[9,10] Since enzymes such as glutathione reductase and cysteine reductase can easily reduce the respective disulfides into thiols using proton sources, combining the features of the manganese complexes and the enzymes into one may convert H$^+$ into H$_2$ without sacrificing thiols in the process through the reversible dissociation and formation of the S-S and S-H bonds.

In this report, we show that an easily-prepared dimanganese disulfide hexacarbonyl complex, [(Mn(CO)$_3$)$_2$(μ-SC$_6$H$_4$-o-S-S-C$_6$H$_4$-o-μ-S-)] (complex **1,** see Scheme 1) can catalyze electrochemical proton reduction using acetic acid as the proton source through the initial reduction of redox-active sulfur atoms of the internal disulfide bond of the complex. The mechanism of the proton reduction process is also investigated by cyclic voltammetry, infrared spectroscopy and density functional theory (DFT) calculations.
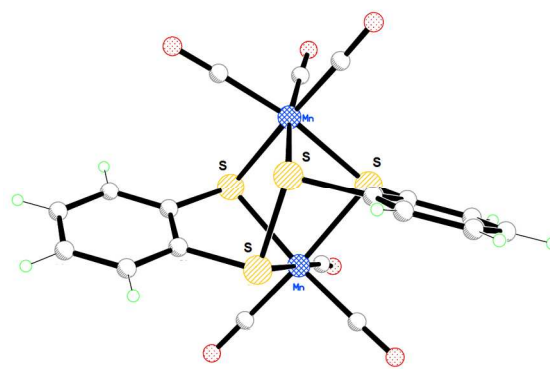

Scheme 1. The structure of complex **1**.

Although the synthesis of **1** has been reported before, a simpler way of preparing **1** is used here instead.[11] Broadband UV photolysis of decacarbonyldimanganese Mn$_2$(CO)$_{10}$ with two equivalent of 1,2-benzenedithiol in hexane for 2 hours generates brown **1** in good yield. Suitable crystals of **1** are grown in dichloromethane/hexane solvent and stored at low temperatures before being subjected to X-ray diffraction (see Supporting Information). As the X-ray crystal structure of **1** has already been described previously, only the salient features of the structure are mentioned.[11] Complex **1** consists of two six-coordinate Mn(I) atoms where each manganese center is coordinated to three sulfur atoms and three terminal carbonyl groups in a distorted octahedral geometry. The internal disulfide bond length in complex **1** of 2.2061(7)Å (see Supporting Information), is significantly longer than the free disulfide bond in diphenyl disulfide bond (2.02Å).[12] There is no Mn-Mn bond as the distance between the two metal centers is too far at around 3.35 Å. Each of the two Mn centers is formally in the +1 oxidation state. The Mn(CO)$_3$ moiety adopts a near-C$_{3v}$ symmetry about the metal center as reflected in the ν$_{CO}$ infrared spectrum (1944, 1965, 2022, 2041 cm^{-1} in CH$_3$CN solvent).
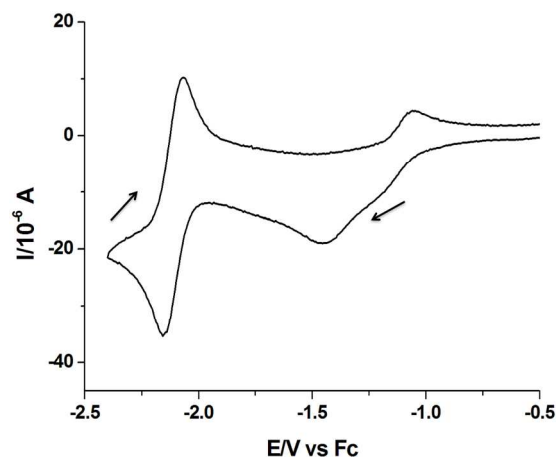
Fig. 1 Cyclic voltammograms of **1** (1 mM) in 0.1 M Bu$_4$NPF$_6$ in DMF at a scan rate of 100 mV/sec. 3 mm glassy-carbon working electrode, platinum counter electrode at 295 K.

The cyclic voltammetric diagram of **1** in DMF in the absence of acid shows three reduction peaks at -1.11 V, -1.38 V and -2.10 V vs Fc$^+$/Fc (Figure 1). Instead of acetonitrile, DMF is the solvent of choice for cyclic voltammetry studies because of the much greater solubility of **1** in DMF. Drawing analogy to a previous study on an organic disulfide,[13] the first peak is assigned to the disulfide bond being reduced by one electron at -1.11V vs Fc$^+$/Fc to the radical anion complex **1**$^-$ (Scheme 2). At -1.38V vs Fc$^+$/Fc, reduction of **1**$^-$ by a second electron to a dianion complex **1**$^{2-}$ occurs. We believe that this complex dissociates to form a monomanganese anion complex **2**$^-$, a previously-detected stable ionic complex.[11] Complex **2**$^-$ can be further reduced by an electron to form another monomanganese complex **2**$^{2-}$ at -2.10V vs Fc$^+$/Fc.[14] Only the third step is observed to be reversible. Further evidence for the formation of **2**$^-$ and its reactions will be discussed later.
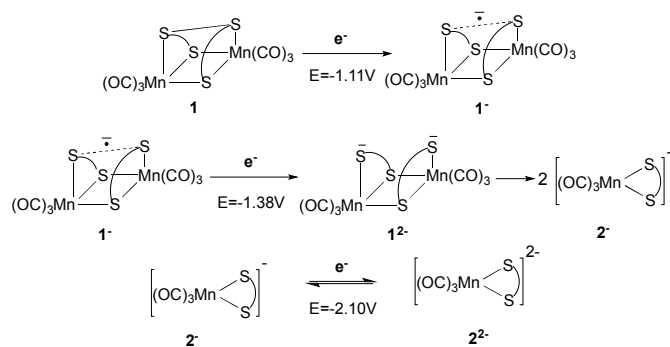
Scheme 2. Proposed pathways for the electroreduction of complex **1**.

The DFT (B3LYP/6-31+G(d)) calculations also support these proposed electroreduction pathways. The Mulliken charge of each of the two sulfur atoms of the disulfide bond changes from 0.205 to

0.058 to -0.116 in complex **1**, **1**$^-$, **1**$^{2-}$ respectively. However, the corresponding Mulliken charge of Mn in each of the three complexes changes very slightly, hence suggesting that the disulfide bond is reduced instead of the manganese. The LUMO calculated for **1** is shown in Figure 2. It shows a mixture of aromatic ring character and antibonding character between the sulfur atoms, which would promote S−S bond cleavage upon electron occupation. The calculated disulfide bond is 2.28 Å, in good agreement with the experimental value. Indeed, the first electron upon reduction goes into the SOMO orbital of **1**$^-$ which is dominated by S−S antibonding character and causes the S−S distance to lengthen from 2.28 Å to 3.10 Å. The second electron upon reduction further lengthens the
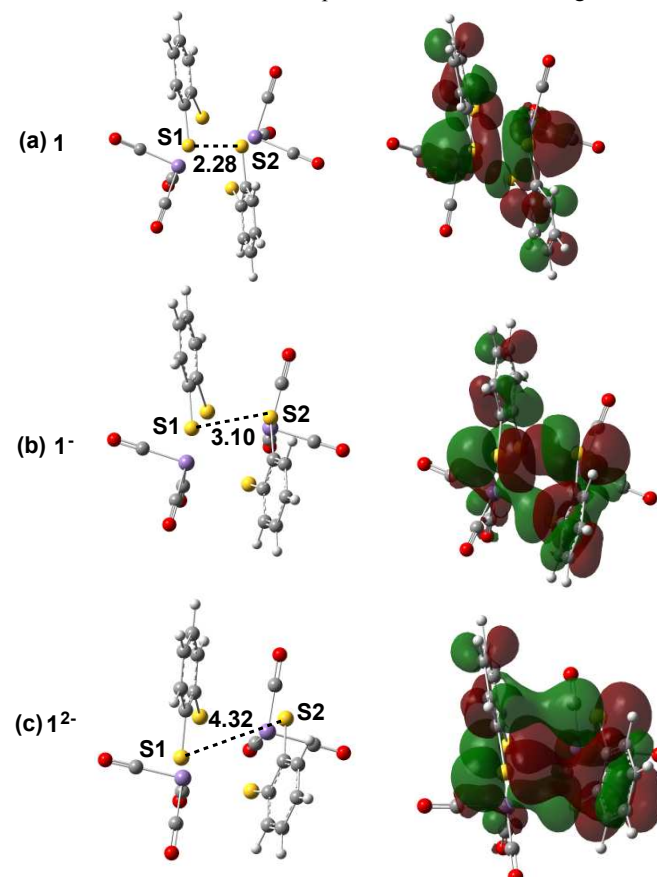
disulfide bond in **1**$^{2-}$ to 4.32 Å after which **1**$^{2-}$ is expected to dissociate to form **2**$^-$. The dissociation of 2- to two **1**$^{2-}$ species is supported by the large computed exoergicity value of -54.4 kcal per mol of 1^{2-}.

Fig. 2 (a) LUMO (lowest unoccupied molecular orbital) of **1** (b) SOMO (singly occupied molecular orbital) of **1**$^-$ (c) HOMO (highest occupied molecular orbital) of **1**$^{2-}$. Color representations: grey is for carbon, white is for hydrogen, red is for oxygen, yellow is for sulfur, purple is for manganese. Bond lengths are shown in Å.

The electroreduction of protons by complex **1** carried out under anaerobic conditions is discussed next. A control experiment is first carried out to determine the potential at which acetic acid in DMF is reduced without the catalyst. However, no peaks were observed even when the potential (vs Fc^+/Fc) is scanned to -2.5V. In contrast, when 5 equivalent amount of CH_3COOH is added into the DMF solution containing **1**, the peak at -2.10V increases dramatically. This peak increases in intensity and shifts gradually to -2.20V as more acid is added. However, the positions of the first two reduction peaks at -
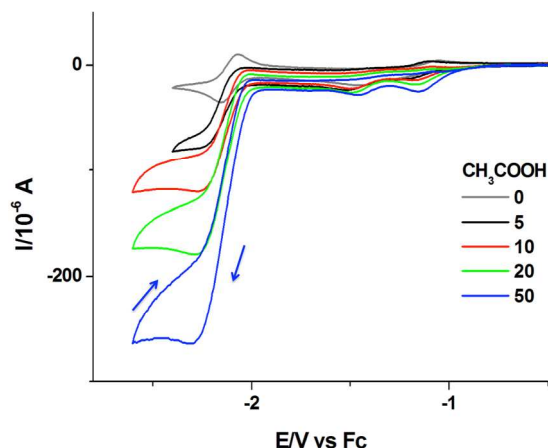
1.11V and -1.38V remain unaffected. The potential at -2.10 V is thus attributed to the catalytic proton reduction potential of **1**, which corresponds to an overpotential of 0.55-0.65 V (CH_3COOH standard reduction potential in DMF is at -1.55 V vs Fc^+/Fc).[15] The electrocatalytic H_2 production was further confirmed by bulk electrolysis of **1** with excess CH_3COOH in DMF at -2.10 V vs Fc^+/Fc with a Faraday yield consistently above 80% in a series of runs.

Fig. 3 Cyclic voltammograms of **1** (1 mM) with CH_3COOH (0−50 mM) in 0.1 M Bu_4NPF_6 in DMF at a scan rate of 100 mV/ sec. 3 mm glassy-carbon working electrode, platinum counter electrode at 295 K.

To further understand the cyclic voltammogram, stoichiometric reactions involving complex **1** are carried out in acetonitrile solvent. Upon addition of $NaBH_4$, the color of the solution changes from brown to red immediately. The v_{CO} peaks of **1** at 1944, 1965, 2022, 2041 cm^{-1} disappear and are replaced by four new peaks at 1895, 1916, 1992 and 2010 cm^{-1} (Figure 4). Following a previous report, the two new peaks at 1895 and 1992 cm^{-1} have been assigned to the sodium salt of **2⁻**, $Na^+[Mn(CO)_3(-SC_6H_4-o-S-)]^-$.[11] The other two peaks at 1916 and 2010 cm^{-1} have been tentatively attributed to the sodium salt of **1²⁻** dimer, which is the likely precursor to **2⁻**. Complex **1²⁻** appears unstable over unstable over a few minutes causing its two peaks to gradually disappear while at the same time the signals of **2⁻** increase slightly in intensity. We have also carried out cyclic voltammetric studies on the solution containing **2⁻**. Indeed a single reversible reduction peak around -2.10V is observed (see Supporting Information), which matches very well with the third reduction peak in the cyclic voltammetry diagram of complex **1**. As reported, addition of a strong acid such as HBF_4 to **2⁻** regenerates the initial four peaks of complex **1** with concomitant H_2 gas evolution.[11]
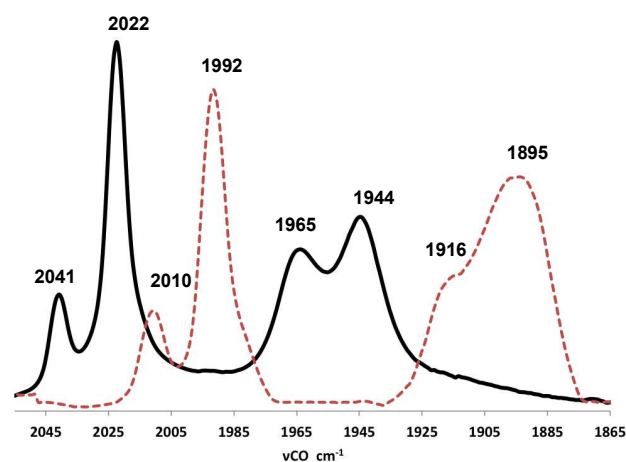

However acetic acid addition does not reverse the reaction, although this observation is consistent with our cyclic voltammetry data interpretation whereby proton reduction using acetic acid as the source does not take place immediately after **2⁻** is generated at the second reduction peak of -1.38 V.

The mechanism of proton reduction by complex **1** is proposed here (see Scheme 3). As discussed previously, complex **1** can be reduced

Fig. 4 FTIR spectra of v_{CO} of complex **1** in CH_3CN (black solid line) and of the products ($Na^+[Mn(CO)_3(-SC_6H_4-o-S-)]^-$ (1895 and 1992 cm^{-1}) and $Na_2^+[(Mn(CO)_3)_2(\mu-SC_6H_4-o-S-S-C_6H_4-o-\mu-S-)]^{2-}$) (1916 and 2010 cm^{-1}) upon $NaBH_4$ addition (red dotted line).

to eventually generate the dianionic monomanganese complex **2²⁻**. The reduction is facilitated by taking place at the S atoms of an elongated disulfide bond within **1**. Upon addition of acetic acid, **2²⁻** is protonated to form either **2H$_S^-$** or **2 H$_M^-$**. The proton is coordinated to one of the sulfur atoms in the former complex or to the Mn center in the latter one. Regardless of the initial proton coordination, we propose that hydride transfer from sulfur to manganese or vice-versa takes place in a facile manner. Either isomer is further protonated to form a common neutral intermediate **2H$_S$H$_M$**. The subsequent interaction between the two coordinated H atoms eventually produces dihydrogen via a complex **2HH** and leaves behind a 16-electron neutral intermediate **2**. Finally, the dimerization of two intermediate **2** regenerates complex **1**.

Scheme 3. Proposed mechanism for the proton reduction process.

Dalton Transactions Accepted Manuscript
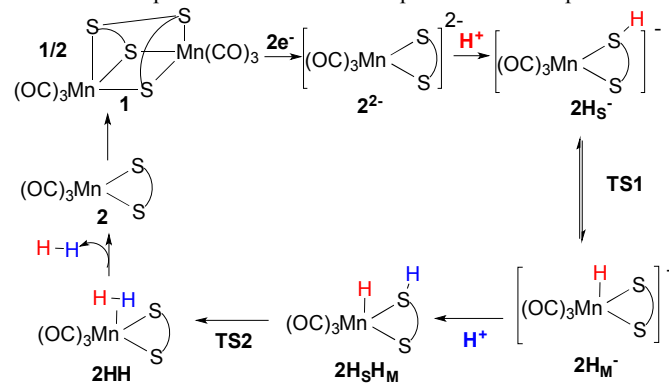
Further support for the proposed mechanism is obtained from DFT calculations. The structures of the complexes are first optimized using B3LYP/6-31+G(d) level of theory. Then single-point energy calculation incorporating a solvation model at both B3LYP/6-311++G(d,p) with SMD//B3LYP/6-31G(d) or M06/6-311++G(d,p) with SMD//M06/6-31G(d)) levels of theory is carried out on the optimized structures.[16] Two important features of the mechanism are explored in more detail. The first study shows that the **2H$_S$⁻** and **2H$_M$⁻** isomers are energetically similar and can perhaps interconvert at room temperature. The free energy diagram in Figure 5a shows the transition state **TS1** of the isomerization between **2H$_S$⁻** and **2H$_M$⁻**. Intermediate **2H$_S$⁻** undergoes intramolecular hydrogen shift from sulfur to manganese through **TS1** with a small energy barrier (6.1(*5.9*) kcal/mol) to form **2H$_M$⁻**, which itself is 4.0(*3.9*) kcal/mol more stable than 2H$_S$⁻. The distance of the S-H bond lengthens from 1.36Å to 1.60 Å while the Mn-H distance shortens from 1.72 Å in **TS1** to 1.60 Å in **2H$_M$⁻**. In the second part of the calculation, we show that the formation of dihydrogen from **2H$_S$H$_M$** is exogernic and also with a small activation barrier. The free energy diagram of **2H$_S$H$_M$** to **2HH** through the transition state **TS2** is shown in Figure 5(b). The distance between the two H1 and H2 atoms shortens from 2.60 Å to 1.29Å in **TS2** with a 7.9(*9.3*) kcal/mol energy barrier with respect to **2H$_S$H$_M$**. The intermediate **2HH** is 9.4(*9.7*) kcal/mol more stable than **2H$_S$H$_M$**.
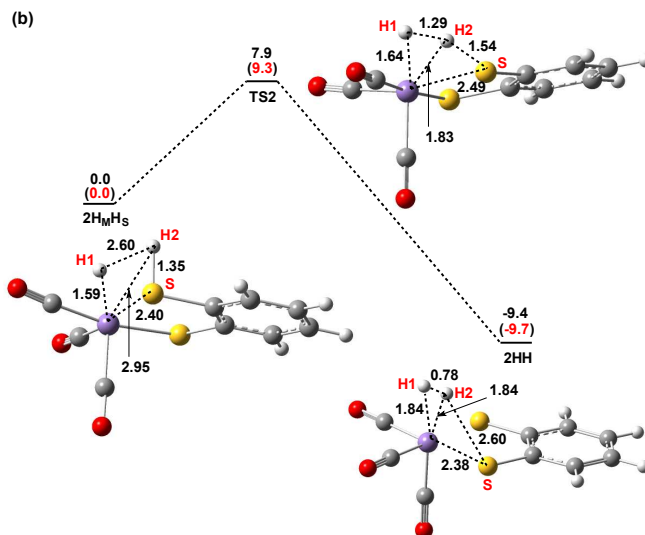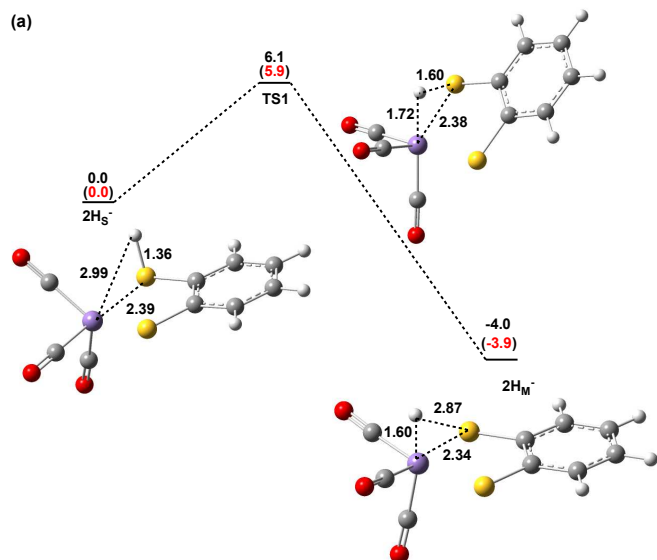
Fig. 5 (a) Free energy diagram of 2H$_S$⁻ to 2H$_M$⁻ through TS1. (b) Free energy diagram of 2H$_S$H$_M$ to 2HH through TS2. Energies are given in kcal/mol (black font: B3LYP functional; red font: M06 functional). Color representations: grey is for carbon, white is for hydrogen, red is for oxygen, yellow is for sulfur, purple is for manganese. Bond lengths are shown in Å.

In summary, a dimanganese hexacarbonyl complex containing a disulfide bond has been used to catalyse proton reduction at overpotentials of 0.55 to 0.65V with acetic acid acting as the proton source. The reduction takes place at the sulfur atoms of the disulfide bond which in turn dissociates 1 into anionic monomanganese complexes. Protonation of these complexes eventually affords H$_2$ gas and regenerates 1, thus completing the catalytic cycle.

Notes and references

1 Peters, J. W.; Lanzilotta, W. N.; Lemon, B. J.; Seefeldt, L. C. *Science* 1998, **282**, 1853.

2 Felton, G. A. N.; Mebi, C. A.; Petro, B. J.; Vannucci, A. K.; Evans, D. H.; Glass, R. S.; Lichtenberger, D. L. *J. Organomet. Chem.* 2009, **694**, 2681.

3 Tard, C.; Pickett, C. J. *Chem. Rev.* 2009, **109**, 2245.

4 Gloaguen, F.; Rauchfuss, T. B. *Chem. Soc. Rev.* 2009, **38**, 100.

5 Felton, G. A. N.; Vannucci, A. K.; Chen, J.; Lockett, L. T.; Okumura, N.; Petro, B. J.; Zakai, U. I.; Evans, D. H.; Glass, R. S.; Lichtenberger, D. L. *J. Am. Chem. Soc.* 2007, **129**, 12521.

6 Zaffaroni, R.; Rauchfuss, T. B.; Gray, D. L.; De Gioia, L.; Zampella, G. *J. Am. Chem. Soc.* 2012, **134**, 19260.

7 Barton, B. E.; Rauchfuss, T. B. *J. Am. Chem. Soc.* 2010, **132**, 14877.

8 Gordon, J. C.; Kubas, G. J. *Organometallics.* 2010, **29**, 4682.

9 Tan, K. Y. D.; Kee, J. W.; Fan, W. Y. *Organometallics.* 2010, **29**, 4459.

10 Tan, K. Y. D.; Teng, G. F.; Fan, W. Y. *Organometallics.* 2011, **30**, 4136.

11 (a) Liaw, W.-F.; Hsieh, C.-K.; Lin, G.-Y.; Lee, G.-H. *Inorg. Chem.* 2001, **40**, 3468. (b) Lee, C.-M.; Lin, G.-Y.; Hsieh, C.-H.; Hu, C.-H.; Lee, G.-H.; Peng, S.-M.; Liaw, W.-F. *J. Chem. Soc. Dalton Trans.* 1999, 2393.

12 Begum, N.; Hyder, M. I.; Kabir, S. E.; Hossain, G. M. G.; Nordlander, E.; Rokhsana, D.; Rosenberg, E. *Inorg. Chem.* 2005, **44**, 9887.

13 Hall, G. B.; Kottani, R.; Felton, G. A. N.; Yamamoto, T.; Evans, D. H.; Glass, R. S.; Lichtenberger, D. L. *J. Am. Chem. Soc.* 2014, **136**, 4012−4018

14 Ray, K.; Bill, E.; Weyhermüller, T.; Wieghardt, K. *J. Am. Chem. Soc.* 2005, **127**, 5641.

15 Felton, G. A. N.; Glass, R. S.; Lichtenberger, D. L.; Evans, D. H. *Inorg. Chem.* 2006, **45**, 9181

16 Marenich, A.V.; Cramer, C.J.; Truhlar, D.G., *J. Phys. Chem. B.* 2009, **113**, 6378